THE JOURNAL OF BIOLOGICAL CHEMISTRY VOL. 292, NO. 5, pp. 2009–2020, February 3, 2017

Down-regulation of Insulin Receptor Substrate 1 during Hyperglycemia Induces Vascular Smooth Muscle Cell Dedifferentiation*

Received for publication, September 15, 2016, and in revised form, December 14, 2016 Published, JBC Papers in Press, December 21, 2016, DOI 10.1074/jbc.M116.758987

Gang Xi[‡], Christine Wai[‡], Morris F. White[§], and David R. Clemmons[‡1]

From the [‡]Division of Endocrinology, Department of Medicine, University of North Carolina School of Medicine, Chapel Hill, North Carolina 27599 and the [§]Division of Endocrinology, Department of Medicine, Children's Hospital, Harvard Medical School, Boston, Massachusetts 02115

Edited by Jeffrey E. Pessin

Diabetes is a major risk factor for the development of atherosclerosis, but the mechanism by which hyperglycemia accelerates lesion development is not well defined. Insulin and insulin-like growth factor I (IGF-I) signal through the scaffold protein insulin receptor substrate 1 (IRS-1). In diabetes, IRS-1 is down-regulated, and cells become resistant to insulin. Under these conditions, the IGF-I receptor signals through an alternate scaffold protein, SHPS-1, resulting in pathophysiologic stimulation of vascular smooth muscle cell (VSMC) migration and proliferation. These studies were undertaken to determine whether IRS-1 is functioning constitutively to maintain VSMCs in their differentiated state and, thereby, inhibit aberrant signaling. Here we show that deletion of IRS-1 expression in VSMCs in non-diabetic mice results in dedifferentiation, SHPS-1 activation, and aberrant signaling and that these changes parallel those that occur in response to hyperglycemia. The mice showed enhanced sensitivity to IGF-I stimulation of VSMC proliferation and a hyperproliferative response to vascular injury. KLF4, a transcription factor that induces VSMC dedifferentiation, was up-regulated in IRS-$1^{-/-}$ mice, and the differentiation inducer myocardin was undetectable. Importantly, these changes were replicated in wild-type mice during hyperglycemia. These findings illuminate a new function of IRS-1: that of maintaining cells in their normal, differentiated state. Because IRS-1 is down-regulated in states of insulin resistance that occur in response to metabolic stresses such as obesity and cytokine stimulation, the findings provide a mechanism for understanding how patients with metabolic stress and/or diabetes are predisposed to developing vascular complications.

Diabetes is a major predisposing factor for the development of atherosclerosis. The diabetes control complications trial showed that patients with type 1 diabetes who maintained a hemoglobin A-1 C value 1.2% lower than control subjects for 7 years had a significantly reduced rate of vascular disease events during the 20-year follow-up period (1). Similarly the United Kingdom prospective trial demonstrated a significant benefit of lowering glucose in type 2 diabetics on cardiovascular risk (2). Despite intense analysis, the molecular mechanism by which glucose lowering results in a clinical benefit has remained poorly defined. Insulin and insulin-like growth factor I (IGF-I)[2] signal through a scaffold protein termed insulin receptor substrate 1 (IRS-1) (3). The insulin and IGF-I receptor tyrosine kinases directly phosphorylate IRS-1, and these phosphotyrosines recruit the p85 subunit of PI3K and Grb-2, thereby activating the PI3K and MAPK pathways (4). In differentiated cells, these IRS-1-linked signaling cascades promote glucose influx; glycogen, lipid, and protein synthesis; as well as changes in gene expression (5). Under normal physiologic conditions, both insulin and IGF-I stimulate differentiated cell functions through IRS-1 activation (6–7). In response to hyperglycemia, proinflammatory cytokines, or nutrient excess, IRS-1 is down-regulated in multiple tissues, and insulin signaling is impaired (8–9). In cell types that are capable of undergoing dedifferentiation, such as vascular smooth muscle cells (VSMCs) and endothelial cells, IGF-I utilizes an alternative mechanism to stimulate PI3K and MAPK activation (10). IGF-I stimulates tyrosine phosphorylation of the scaffolding protein Src homology 2 domain-containing protein tyrosine phosphatase substrate 1 (SHPS-1), which recruits signaling elements that activate both the PI3K and MAPK pathways, leading to enhanced cell migration and proliferation (11). In contrast, under the same hyperglycemic conditions, overexpression of IRS-1 down-regulates SHPS-1 expression, thereby restoring signaling through IRS-1, which inhibits these pathophysiologic changes (12). Dedifferentiation of VSMCs has been implicated as a major event in atherosclerotic lesion formation (13). Several signaling events by which external stimuli such as hyperlipidemia and cytokine expression control differentiation have been reported, but the changes in signaling that lead to dedifferentiation of VSMCs during hyperglycemia have not been characterized. Based on those observations, we investigated whether IRS-1-mediated signaling was required to maintain VSMC differentiation and whether decreased expression of IRS-1 led to dedifferentiation and altered sensitivity to stimulation of cell proliferation.

* This work was supported by National Institutes of Health Grants AG02331 and EY021943. The authors declare that they have no conflicts of interest with the contents of this article. The content is solely the responsibility of the authors and does not necessarily represent the official views of the National Institutes of Health.

[1] To whom correspondence should be addressed: CB#7170, 8024 Burnett-Womack, Div. of Endocrinology, University of North Carolina, Chapel Hill, NC 27599-7170. Tel.: 919-966-4735; Fax: 919-966-6025; E-mail: david_clemmons@med.unc.edu.

[2] The abbreviations used are: IGF, insulin-like growth factor; IRS, insulin receptor substrate; VSMC, vascular smooth muscle cell; AKT, protein kinase B; PCNA, proliferating cell nuclear antigen; UNC, University of North Carolina.

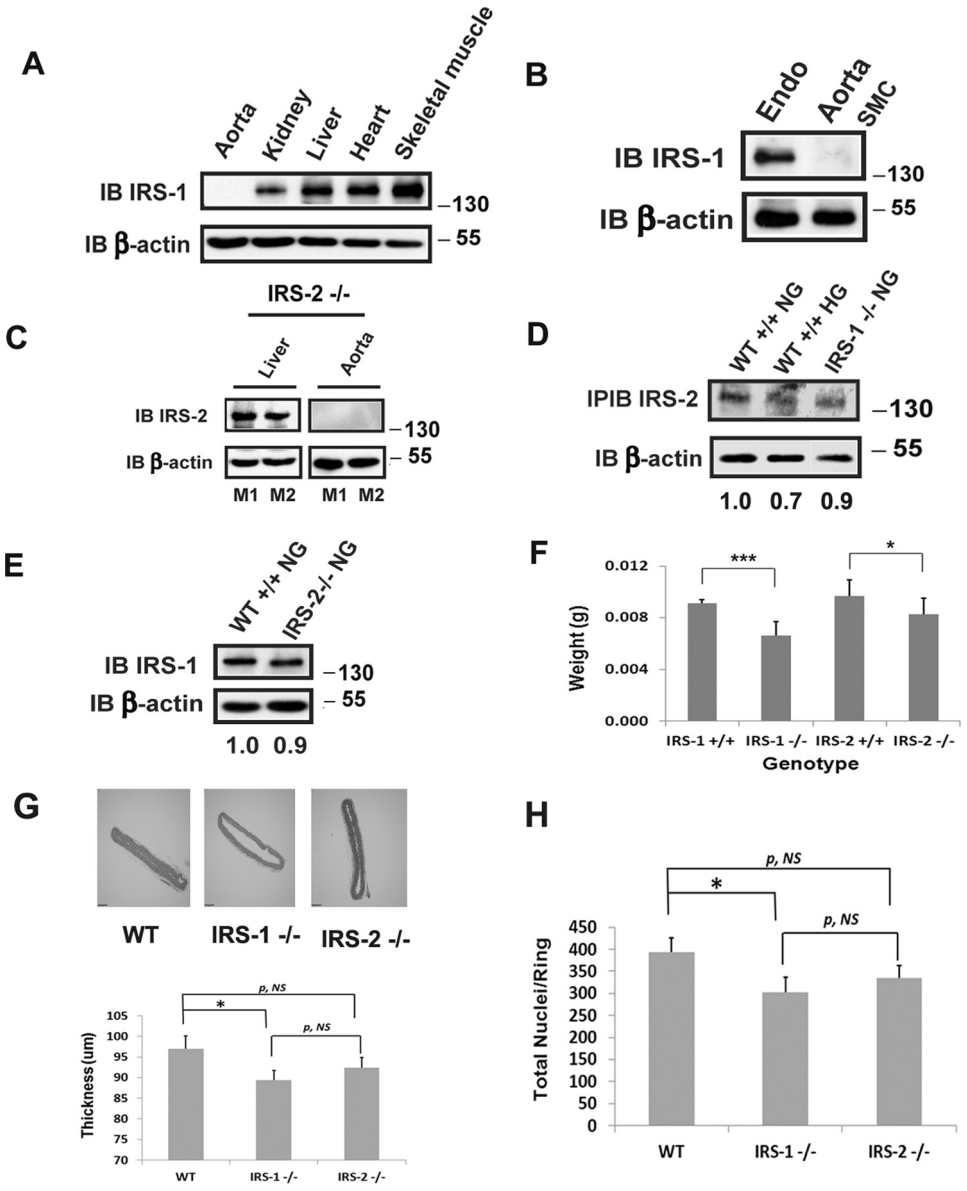

FIGURE 1. **Deletion of IRS-1 or IRS-2 expression in vascular smooth muscle from mouse aorta.** IRS-1 or IRS-2 smooth muscle-specific knockout mice were generated following a procedure described under "Experimental Procedures." *A*, 15-week-old IRS-1 smooth muscle-specific knockout mice were sacrificed, and aortae as well as the organs listed were removed. Organ and tissue extracts were prepared as under "Experimental Procedures," immunoblotted (*IB*) with an anti-IRS-1 antibody, and reprobed with an anti-β-actin antibody. *B*, aortas were cleaned by removing the connective tissue and the adventitia under the dissecting microscope. The cleaned aortas were opened longitudinally, and the endothelium (*Endo*) was collected in the PBS by gently scraping with a scalpel. The endothelia from nine aortae were pooled and then lysed using a modified radioimmunoprecipitation assay buffer. The remaining SMCs were analyzed separately. The lysates were immunoblotted as in *A*. *C*, 15-week-old IRS-2 smooth muscle-specific knockout mice were sacrificed, and aortic or hepatic lysates were prepared as described under "Experimental Procedures." The tissue lysates were immunoblotted with an anti-IRS-2 antiserum and reprobed with an anti-β-actin antibody. *M1* and *M2* denote two representative mice. *D*, aortic extracts from normal wild-type ($WT^{+/+}$ *NG*, $n = 4$), diabetic wild-type ($WT^{+/+}$ *HG*, $n = 4$), and normal IRS-1 knockout ($IRS\text{-}1^{-/-}$ *NG*, $n = 4$) mice were immunoprecipitated and immunoblotted with an anti-IRS-2 antibody. The same amount of extract was immunoblotted with an anti-β-actin antibody to control for protein loading. The ratio value of the scanning units for IRS-2 divided by the scanning units of corresponding β-actin from the first lane ($WT^{+/+}$ *NG*) was set as 1.0, and the values of other lanes were obtained from the ratio value of the corresponding lane divided by the ratio value of the first lane. *E*, aortic extracts from normal wild-type ($WT^{+/+}$ *NG*, $n = 4$) and IRS-2 knockdown ($IRS\text{-}2^{-/-}$ *NG*, $n = 4$) mice were immunoblotted with anti-IRS-1 and anti-β-actin antibodies. The ratio value of the scanning units for IRS-1 divided by the scanning units of corresponding β-actin from the first lane ($WT^{+/+}$ *NG*) was set as 1.0, and the value of the second lane was obtained from the ratio value of the second lane ($IRS\text{-}2^{-/-}$ *NG*) divided by the ratio value of the first lane. *F*, aortae were removed from IRS-1 or IRS-2 smooth muscle-specific knockout mice or their wild-type littermates, and the adventitia was removed under a dissecting microscope before weighing. *G*, sections of aortae from WT or IRS-1 or IRS-2 smooth muscle-specific knockout mice were stained with hematoxylin and eosin, and images were captured using an Olympus BX61 microscope. The aortic thickness was measured following the procedure described under "Experimental Procedures." *H*, the same sections as in *G* were stained with DAPI following the procedure described under "Experimental Procedures." The total nuclei were counted in each group. ***, $p < 0.001$; *, $p < 0.05$; significant differences between mouse genotypes. *NS*, no significant difference between two treatments. *Error bars* denote the standard deviation.

Results

To determine the effect of loss of expression of IRS-1, we prepared mice in which expression had been selectively deleted in VSMCs. As shown in Fig. 1, IRS-1 expression was eliminated in VSMCs but not in the liver, kidney, heart, skeletal muscle (Fig. 1*A*), or endothelium (Fig. 1*B*). Similarly, IRS-2 was selec-

tively deleted in the aorta but not in the liver (Fig. 1*C*). Furthermore, no compensatory increase in IRS-2 expression was detected in the aortas of IRS-$1^{-/-}$ mice and vice versa (Fig. 1, *D* and *E*). There was no difference in body weight or organ size among the groups. However, smooth muscle-specific deletion of IRS-1 or IRS-2 resulted in a significant reduction in the weight of the aorta compared with control animals, and the effect of IRS-1 deletion was significantly greater than deleting IRS-2 (Fig. 1*F*). Similar results were obtained when the aortic wall thickness (*e.g.* control, 97 ± 3; IRS-$1^{-/-}$, 89 ± 2; IRS-$2^{-/-}$, 92 ± 3 μm) and total nuclei (*e.g.* control, 393 ± 32; IRS-$1^{-/-}$, 303 ± 33; IRS-$2^{-/-}$, 334 ± 30) in the aortic ring sections were analyzed (Fig. 1, *G* and *H*). These results are consistent with the known effects of IRS-1 and IRS-2 in mediating fetal growth (4).

Our prior studies have shown that, in response to hyperglycemia and IRS-1 down-regulation, the transmembrane protein SHPS-1 is up-regulated and functions to transduce IGF-I signaling (10–11). The IGF-I receptor phosphorylates SHPS-1, which forms a scaffold for signaling complex localization, and this complex mediates IGF-I actions in VSMCs during hyperglycemia (10, 12). Therefore, we analyzed SHPS-1 complex activation in the different settings. Our results showed that IGF-I stimulated a major increase in SHPS-1 tyrosine phosphorylation in aortae from IRS-1 VSMC knockout non-diabetic mice, and wild-type animals that had been made diabetic showed a similar response, whereas normal control mice showed no change in SHPS-1 phosphorylation (Fig. 2*A*). This change was specific for IRS-1 because IRS-2 VSMC knockout animals showed no SHPS-1 phosphorylation response. In contrast, IRS-1 tyrosine phosphorylation in response to IGF-I could only be detected in normal wild-type and IRS-2 knockout animals (Fig. 2*B*). There was minimal IRS-2 protein, and no IRS-2 tyrosine phosphorylation was detected in control, diabetic, wild-type animals or IRS-1 knockout animals (Fig. 2*C*). This signaling switch was associated with enhanced downstream signaling responses. When the four groups of mice were compared, IGF-I induced 7.5 ± 0.8-fold and 9.3 ± 0.7-fold increases in protein kinase B (AKT) phosphorylation in normoglycemic IRS-$1^{-/-}$ and diabetic (IRS-$1^{+/+}$) animals, respectively, whereas control and IRS-$2^{-/-}$ animals showed minimal changes (Fig. 2, *D* and *E*). When MAPK activation was analyzed, there were 7.0 ± 0.8-fold and 2.7 ± 0.2-fold increases in IRS-$1^{-/-}$ and IRS-$1^{+/+}$ diabetic mice, respectively, and no increase in MAPK activation in IRS-$2^{-/-}$ or control animals (Fig. 2, *D* and *E*). SHPS-1-mediated activation of downstream signaling requires recruitment of SHP-2 to the phosphotyrosines on SHPS-1 (12). SHP-2 recruitment results in assembly of a signaling complex composed of Src, p52 Shc, and Grb-2, which subsequently activates MAPK and AKT (12). Therefore, to confirm that the changes in downstream signaling that occurred in the IRS-$1^{-/-}$ mice were mediated through SHPS-1, we utilized a cell-permeable peptide that disrupts SHP-2/SHPS-1 association (11). The peptide significantly diminished SHP-2 recruitment in diabetic (IRS-$1^{+/+}$) and non-diabetic IRS-$1^{-/-}$ mice (Fig. 3*A*). Importantly, it also inhibited IGF-I induction of AKT and MAPK activation (Fig. 3*B*).

Next we determined the significance of these changes in signaling for cellular replication. IGF-I induced no change in replication in aortae obtained from control animals; however, following IRS-1 deletion, there was a 2.0 ± 0.3-fold increase in Ki67 labeling that was comparable with the 1.6 ± 0.1-fold change that occurred in wild-type diabetic animals (Fig. 4). However, in IRS-2 knockout animals, this increase could only be detected in diabetic animals, and the magnitude of the increase was similar to wild-type animals (1.8 ± 0.6-fold *versus* 1.6 ± 0.1-fold increases). VSMCs in adult animals are capable of undergoing dedifferentiation, and this results in a hyperproliferative response to growth stimuli. Therefore, we determined whether IRS-1 knockdown was associated with a change in VSMC differentiation. As shown in Fig. 5*A*, the transcription factor Kruppel-like factor 4 (KLF-4), which inhibits the expression of genes that stimulate smooth muscle cell differentiation, was significantly increased in the IRS-$1^{-/-}$ mice. This increase was also noted in diabetic animals, but there was no change in wild-type non-diabetic or IRS-$2^{-/-}$ animals. This change was associated with a marked decrease in the expression of myocardin, a protein whose expression is required for VSMC differentiation (13) (Fig. 5*A*), and SM22, a marker of smooth muscle cell differentiation (Fig. 5*D*). Similar to wild-type animals, these changes were only detected in the diabetic animals but not in non-diabetic animals with IRS-2 deletion (Fig. 5, *B* and *E*). Importantly, these changes could be reversed using SHPS-1/SHP-2-disrupting peptide in diabetic wild-type mice and IRS-$1^{-/-}$ mice; that is, KLF4 expression was inhibited, and myocardin and SM22 were stimulated in diabetic and IRS-$1^{-/-}$ animals (Fig. 5, *C* and *F*). This finding strengthens the conclusion that the SHPS-1 signaling pathway predominated under these conditions.

To determine the functional consequences of decreased IRS-1 expression and VSMC dedifferentiation, the three groups of mice were wounded, and VSMC proliferation was determined. There was a major increase in arterial wall thickness in femoral arteries from IRS-$1^{-/-}$ animals (Fig. 6*A*). Quantitative analysis showed a 4.7 ± 0.9-fold increase in IRS-$1^{-/-}$ mice and a 6.6 ± 1.1-fold change in diabetic mice compared with a 2.4 ± 0.6-fold change in control animals. To determine whether this change was in part due to increased proliferation of VSMCs, Ki67 labeling and α-actin were analyzed. There was a 46.3% ± 7.4% increase in IRS-$1^{-/-}$ mice and a 50.3% ± 6.0% increase in diabetic animals (Fig. 6*B*), whereas this change was significantly less (*e.g.* 15.0% ± 5.2%) in control animals. Biochemical analyses verified that KLF4 expression was markedly up-regulated following wounding, and myocardin expression was undetectable in the IRS-$1^{-/-}$ and diabetic mice (Fig. 7*A*). In contrast, there was no change in control animals. Similarly, MAPK and AKT phosphorylation were markedly enhanced in IRS-$1^{-/-}$ mice and the diabetic (IRS-$1^{+/+}$) animals but changed only minimally in the non-diabetic controls (Fig. 7*B*). To determine whether these changes might affect vascular function, several markers, such as SM22, α-actin, and proliferating cell nuclear antigen (PCNA), were analyzed. The results showed that wounding treatment induced PCNA in diabetic wild-type and non-diabetic IRS-$1^{-/-}$ mice, whereas SM22 and α-actin expression were remarkably reduced (Fig. 7*C*).

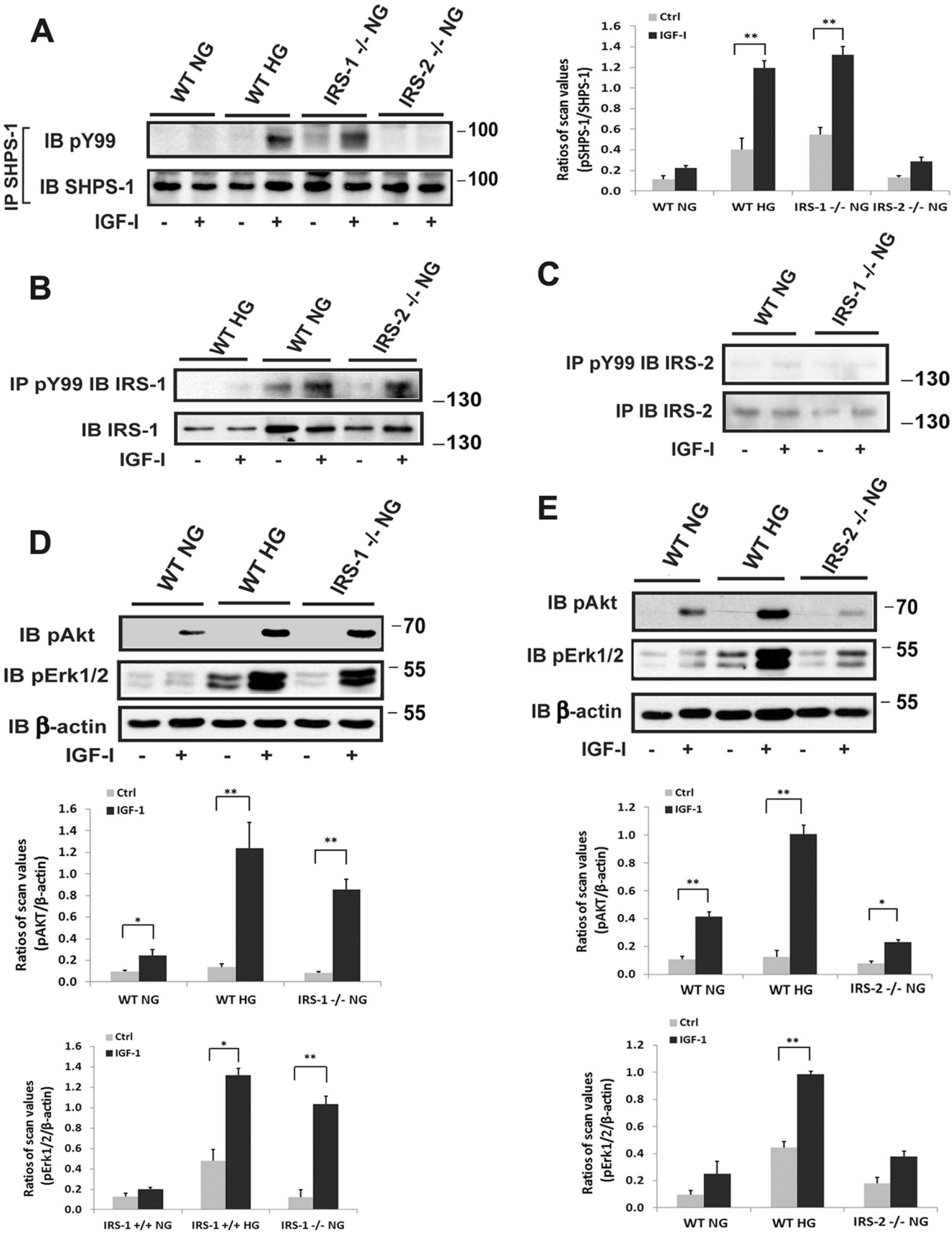
A
WT NG
WT HG
IRS-1 -/- NG
IRS-2 -/- NG
IP SHPS-1
IB pY99
IB SHPS-1
100
100
IGF-I - + - + - + - +
Ctrl
IGF-I
Ratios of scan values (pSHPS-1/SHPS-1)
WT NG
WT HG
IRS-1 -/- NG
IRS-2 -/- NG
B
WT HG
WT NG
IRS-2 -/- NG
IP pY99 IB IRS-1
IB IRS-1
130
130
IGF-I - + - + - +
C
WT NG
IRS-1 -/- NG
IP pY99 IB IRS-2
IP IB IRS-2
130
130
IGF-I - + - +
D
WT NG
WT HG
IRS-1 -/- NG
IB pAkt
IB pErk1/2
IB β-actin
70
55
55
IGF-I - + - + - +
Ctrl
IGF-1
Ratios of scan values (pAKT/β-actin)
WT NG
WT HG
IRS-1 -/- NG
Ratios of scan values (pErk1/2/β-actin)
IRS-1 +/+ NG
IRS-1 +/+ HG
IRS-1 -/- NG
E
WT NG
WT HG
IRS-2 -/- NG
IB pAkt
IB pErk1/2
IB β-actin
70
55
55
IGF-I - + - + - +
Ctrl
IGF-1
Ratios of scan values (pAKT/β-actin)
WT NG
WT HG
IRS-2 -/- NG
Ratios of scan values (pErk1/2/β-actin)
WT NG
WT HG
IRS-2 -/- NG

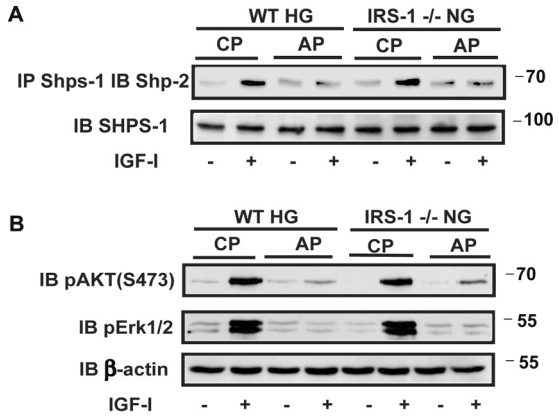

FIGURE 3. **Disruption of SHPS-1 signaling complex formation prevents enhanced IGF-I-dependent MAPK and AKT activation.** *A*, aortic lysates from diabetic wild-type mice (*WT HG*) and normal IRS-1 knockout mice (*IRS-1*$^{-/-}$ *NG*) that had been treated with a control peptide (*CP*) or a SHPS-1/SHP-2-disrupting peptide (*AP*) were immunoprecipitated (*IP*) with an anti-SHPS-1 antibody and immunoblotted (*IB*) with an anti-SHP-2 antibody. The same amount of each aortic lysate was immunoblotted with an anti-SHPS-1 antibody as a loading control. Scanning densitometry values obtained from of the aortic extracts from three mice in two separate experiments showed a 5.8 ± 0.9-fold increase in wild-type diabetic mice exposed to the control peptide and a 1.6 ± 0.3-fold ($p < 0.01$) change with the disrupting peptide. The increases were 6.4 ± 0.7-fold and 1.4 ± 0.2-fold ($p < 0.01$), respectively, in IRS-1$^{-/-}$ mice. *B*, the aortic extracts were immunoblotted with anti-pAKT (Ser-473) and pErk1/2 antibodies. The blots were reprobed with an anti-β-actin antibody to control for loading. The increases AKT activation were 9.5 ± 1.7-fold and 1.7 ± 0.2-fold ($p < 0.001$) in wild-type diabetic and 9.1 ± 1.5-fold compared with 2.0 ± 0.3-fold ($p < 0.01$) in IRS-1$^{-/-}$ mice. The changes in MAPK were 6.0 ± 1.0-fold and 1.2 ± 0.2-fold ($p < 0.01$) in diabetic wild-type mice and 7.9 ± 1.6-fold compared with 1.3 ± 0.3-fold ($p < 0.01$) in IRS-1$^{-/-}$ mice.

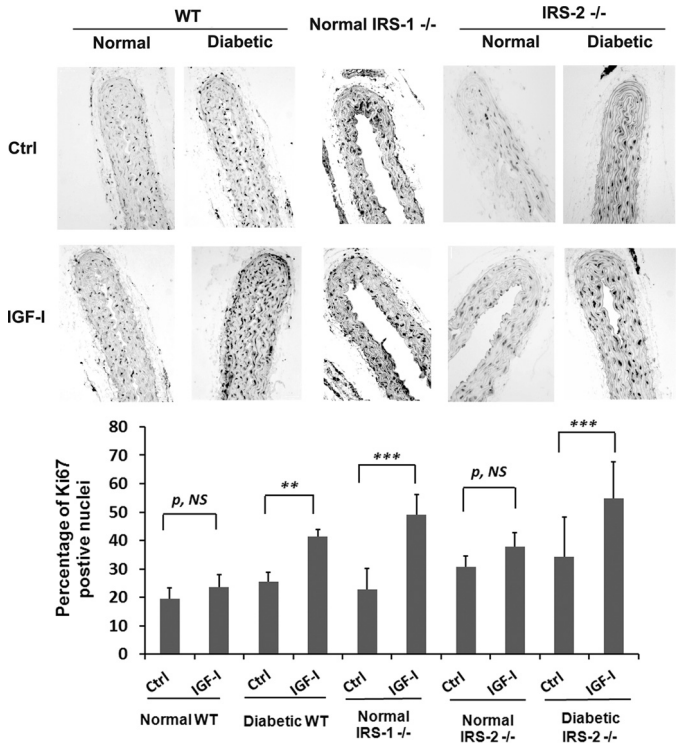

FIGURE 4. **Smooth muscle-specific knockout of IRS-1 enhances IGF-I-stimulated VSMC replication in aortae from normal mice.** Normal WT ($n = 12$), diabetic WT ($n = 12$), normal IRS-1 knockout (*Normal IRS-1*$^{-/-}$, $n = 12$), normal IRS-2 knockout (*Normal IRS-2*$^{-/-}$, $n = 8$), or diabetic IRS-2 knockout (*Diabetic IRS-2*$^{-/-}$, $n = 8$) mice were injected with IGF-I or PBS i.p. twice (24 h and 15 min) before sacrifice. Paraffin-embedded sections were stained with anti-Ki67 antibody and DAPI following the procedures described under "Experimental Procedures," and the number of proliferating cells and total nuclei in the each section (total 30 sections) were counted and expressed as the percentage of Ki67-positive nuclei. The mean values ± S.D. from 6 mice/treatment group (3 sections measured/mouse) are shown graphically, and representative images are also shown. ***, $p < 0.001$; **, $p < 0.01$; significant differences when the two treatments were compared. *NS*, no significant difference between two treatments. *Ctrl*, control.

Discussion

During normoglycemia, adult VSMCs remain differentiated and do not proliferate. Under these conditions, IRS-1 mediates normal physiologic responses following insulin or IGF-I stimulation, including glucose transport, protein synthesis, and inhibition of apoptosis (3). In contrast, during hyperglycemia or insulin-resistant states, IRS-1 is down-regulated (8–10). In cultured VSMCs exposed to high glucose, IGF-I downstream signaling is dysregulated and mediated through the scaffolding protein SHPS-1 (11–12). Overexpression of IRS-1 under these conditions inhibits SHPS-1 tyrosine phosphorylation in response to IGF-I, and this is associated with attenuated VSMC migration and proliferation (12). This study was undertaken to determine whether IRS-1 functions constitutively in a cell-autonomous manner to inhibit these aberrant responses under normoglycemic conditions *in vivo*. The findings demonstrate unequivocally that this signaling switch occurs in intact arteries in mice following deletion of IRS-1 expression. Specifically, in VSMCs, IRS-1 deletion resulted in enhancement of the ability of IGF-I to stimulate SHPS-1 tyrosine phosphorylation during normoglycemia. This function was cell-autonomous and not dependent on deletion of IRS-1 expression in other vascular cell types, such as endothelium. This up-regulation of SHPS-1 tyrosine phosphorylation during normoglycemia resulted in significant enhancement of AKT and MAPK phosphorylation as well as cell proliferation. Of greater importance is that knockdown of IRS-1 led to increased expression of the dedifferentiation-associated transcription factor KLF-4 and down-regulation of myocardin and SM22, two important stimuli of VSMC differentiation. Therefore, we conclude that IRS-1 expression is necessary to maintain VSMCs in their normal, differentiated state. The loss of IRS-1 results in dedifferentiation that is accompanied by aberrant signaling through SHPS-1 and enhancement

FIGURE 2. **Smooth muscle-specific knockout of IRS-1 but not IRS-2 enhances IGF-I signaling in aortae from normal mice.** Aortae from wild-type mice (*WT NG*), diabetic wild-type mice (*WT HG*), non-diabetic IRS-1 (*IRS-1*$^{-/-}$ *NG*) or IRS-2 (*IRS-2*$^{-/-}$ *NG*) VSMC knockout mice that had been injected with IGF-I (+) or PBS (−) (Ctrl) were prepared as under "Experimental Procedures." *A*, aortic lysates were immunoprecipitated (*IP*) with an anti-SHPS-1 antibody and immunoblotted (*IB*) with anti-Tyr(P)-99. The blots were reprobed with an anti-SHPS-1 antibody as a loading control. The value of each column is the ratio of the mean ± S.D. value of the scanning units for pSHPS-1 divided by the scanning units of total SHPS-1. *B* and *C*, aortic lysates were immunoprecipitated with an anti-Tyr(P)-99 antibody and immunoblotted with anti-IRS-1 (*B*) or IRS-2 (*C*). The same amount of lysate was analyzed using an anti-IRS-1 (*B*) or IRS-2 (*C*) antibody as a loading control. *D* and *E*, aortic lysates were immunoblotted with anti-pAKT (Ser-473) or anti-pErk1/2 and reprobed with an anti-β-actin antibody as a loading control. The value of each bar is the ratio of the mean ± S.D. of the scanning units for pAKT or pErk1/2 divided by the scanning units of corresponding β-actin band. *, $p < 0.05$; **, $p < 0.01$; significant differences between IGF-I treatment and the basal level. Each experimental data point represents the mean ± S.D. obtained from two replicates of three mice per treatment.

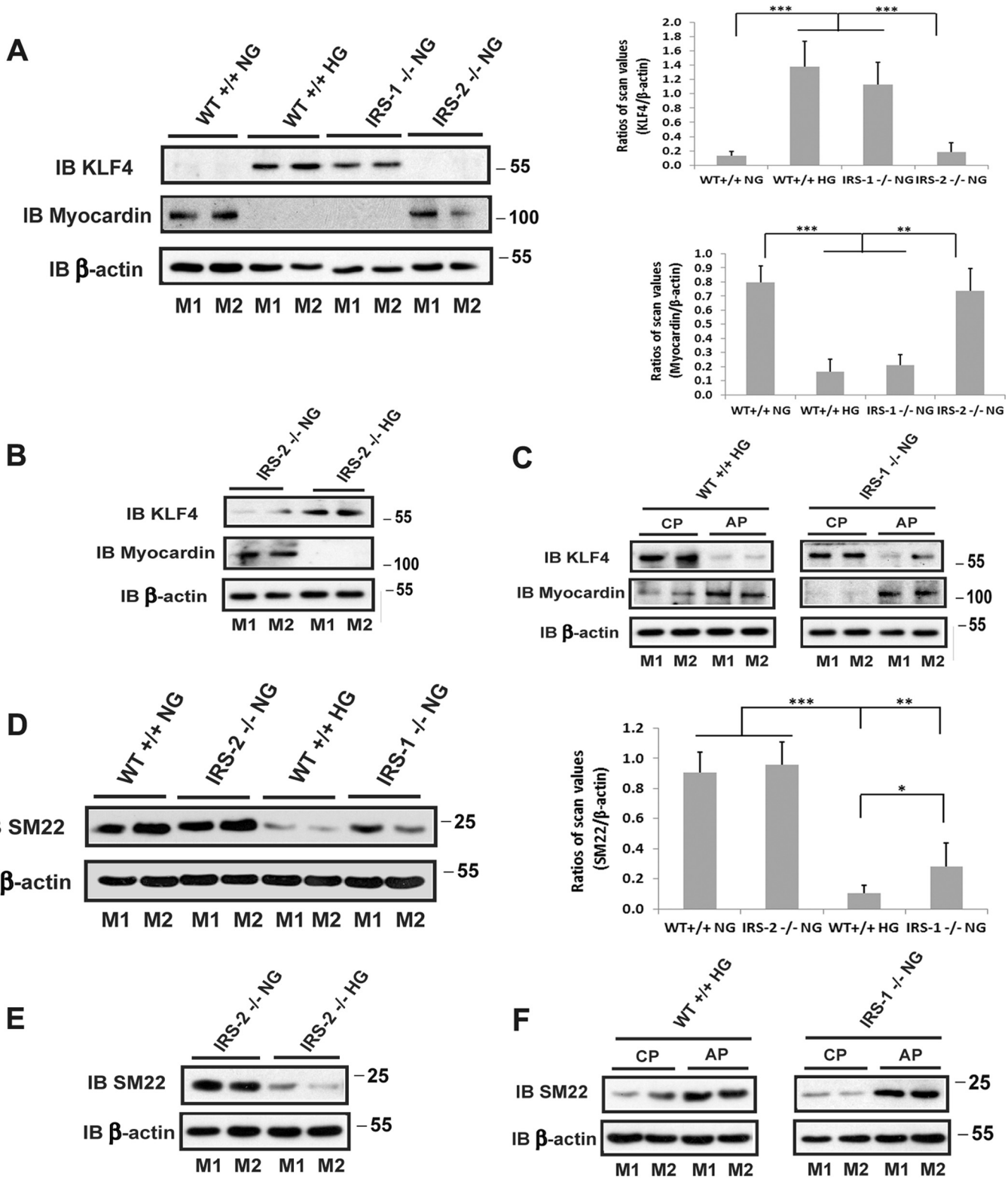

FIGURE 5. **Smooth muscle-specific knockout of IRS-1 but not IRS-2 stimulates the dedifferentiation of aortic smooth muscle cells.** *A*, *B*, *D*, and *E*, aortae from normal wild-type mice ($WT^{+/+}$ *NG*), diabetic wild-type mice ($WT^{+/+}$ *HG*), normal IRS-1 knockout mice ($IRS\text{-}1^{-/-}$ *NG*), IRS-2 knockout mice ($IRS\text{-}2^{-/-}$ *NG*), or diabetic IRS-2 knockout mice ($IRS\text{-}2^{-/-}$ *HG*) were prepared following the procedure described under "Experimental Procedures." The lysates were immunoblotted (*IB*) with anti-KLF4, anti-myocardin (*A* and *B*) or anti-SM22 antibody (*D* and *E*). The blots were reprobed with an anti-β-actin antibody as a loading control. The value of each column is the ratio of the mean ± S.D. value of the scanning units obtained from 6 mice/group for KLF4, myocardin, or SM22 divided by the scanning units of corresponding β-actin, respectively. *, $p < 0.05$; **, $p < 0.01$; ***, $p < 0.001$; significant differences between two mouse types. *C* and *F*, aortic lysates from diabetic wild-type mice ($WT^{+/+}$ *HG*) or non-diabetic IRS-1 knockout mice ($IRS\text{-}1^{-/-}$ *NG*) treated with SHPS-1/SHP2-disrupting peptide (*AP*) or a control peptide (*CP*) for 5 days were immunoblotted with anti-KLF4, anti-myocardin (*C*), or anti-SM22 antibody (*F*). The blots were reprobed with an anti-β-actin antibody as a loading control. *M1* and *M2* denote two representative mice for each group.

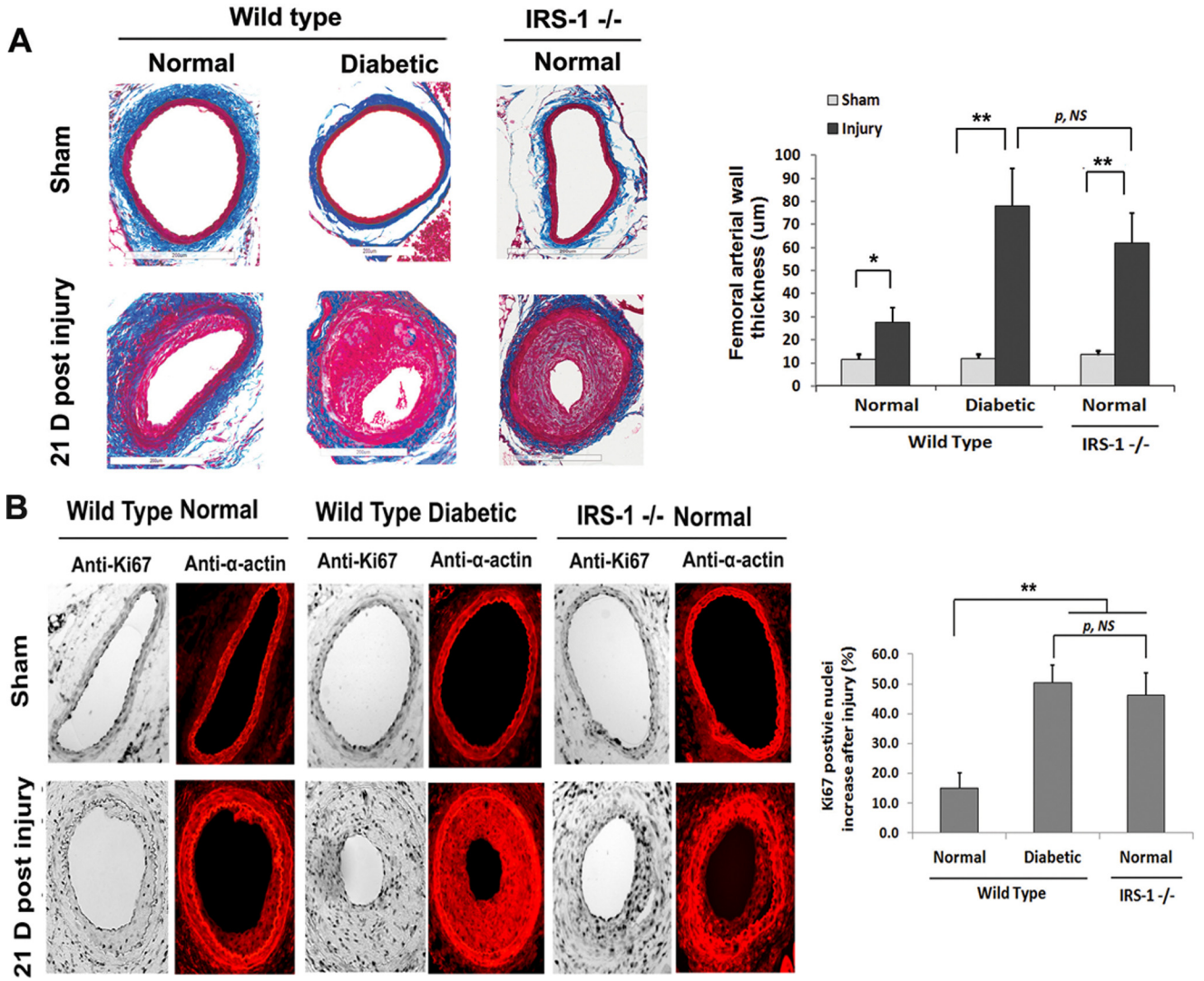

FIGURE 6. **Smooth muscle-specific knockout of IRS-1 enhances femoral arterial cell proliferation after injury.** Femoral arterial sections after injury or sham treatment from normal wild-type, diabetic wild-type, and normal IRS-1$^{-/-}$ mice were prepared following a procedure described under "Experimental Procedures." *A*, the sections were stained with Masson trichome elastin stain, and images were captured and analyzed as under "Experimental Procedures." Representative cross-sections are shown. The value of each column is the mean value ± S.D. obtained from 12 mice from each group. *B*, the sections were stained with anti-Ki67 and anti-α-actin antibodies and DAPI following a procedure described under "Experimental Procedures." The value of each column is the mean value ± S.D. of the percentage increase of Ki67-positive nuclei after injury above the sham treatment value for each mouse group ($n = 12$). **, $p < 0.01$; *, $p < 0.05$; significant differences when the two treatments or two mouse types were compared. *NS*, no significant difference. *Error bars* denote the standard deviation.

of VSMC proliferation in response to IGF-I or vascular injury (Fig. 8).

In addition to SHPS-1 activation, we investigated the possibility that up-regulation of IRS-2 could compensate for loss of IRS-1. However, the results clearly show that, following IRS-1 deletion or induction of diabetes, there is no increase in IRS-2 and that deletion of IRS-2 does not induce SHPS-1 activation in the aorta. Therefore, we conclude that the loss of IRS-1 does not induce IRS-2 and that the switch in signaling that occurs with hyperglycemia from IRS-1 to SHPS-1 is IRS-2-independent.

IRS-1 is down-regulated in multiple cell types in response to hyperglycemia, including VSMCs (11), skeletal muscle (14), endothelium (15), pre-adipocytes (16), hepatocytes (16), and cardiomyocytes (17). Several mechanisms have been postulated to mediate this change, including serine phosphorylation of IRS-1 (18), direct proteolytic degradation (19), and ubiquitination with targeting to proteasomes (20). Multiple serine/threonine kinases, including JNK, mechanistic target of rapamycin (mTOR), MAPK, and several protein kinase C isoenzymes that phosphorylate IRS-1 are activated in response to hyperglycemia (21–22). Cytokine activation of the NF-κB pathway (23), dyslipidemia (24), and hormones that stimulate endothelial dysfunction, such as angiotensin II (25) and aldosterone (26), induce IRS-1 down-regulation, and this is a mechanism by which these factors confer insulin resistance. Whether each of these factors can induce SHPS-1 activation has not been reported, but a recent study showed that TNFα stimulation of skeletal muscle activated SHPS-1 expression and down-regulated IRS-1 (23). In that model, knockdown of SHPS-1 restored insulin signaling and IRS-1 tyrosine phosphorylation. This suggests that there is a dynamic interplay between IRS-1 and SHPS-1 signaling to maintain insulin sensitivity and that dys-

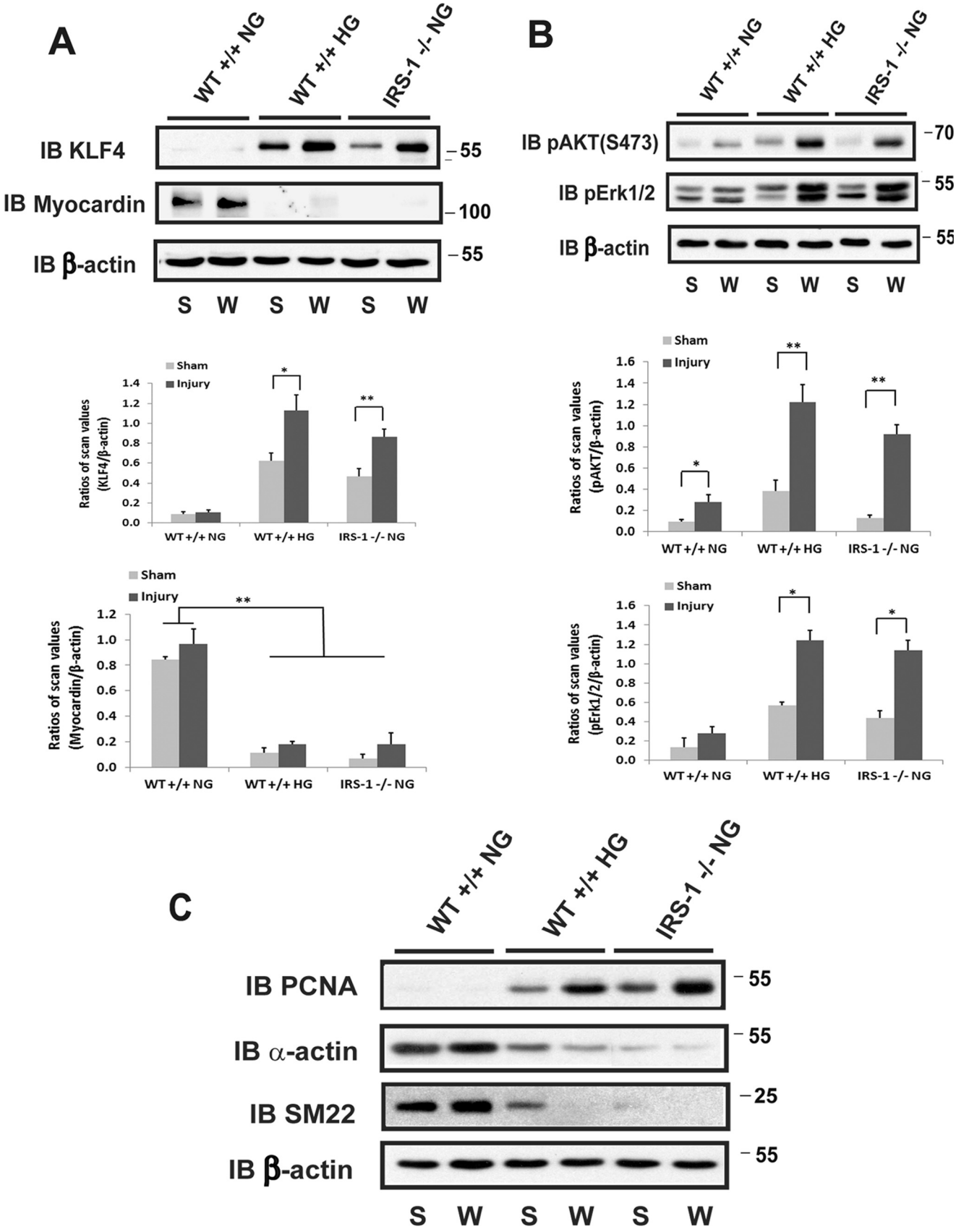
A
WT +/+ NG
WT +/+ HG
IRS-1 -/- NG
IB KLF4
IB Myocardin
IB β-actin
55
100
55
S W S W S W
B
WT +/+ NG
WT +/+ HG
IRS-1 -/- NG
IB pAKT(S473)
IB pErk1/2
IB β-actin
70
55
55
S W S W S W
Sham
Injury
Ratios of scan values (KLF4/β-actin)
Ratios of scan values (Myocardin/β-actin)
Ratios of scan values (pAKT/β-actin)
Ratios of scan values (pErk1/2/β-actin)
WT +/+ NG
WT +/+ HG
IRS-1 -/- NG
C
WT +/+ NG
WT +/+ HG
IRS-1 -/- NG
IB PCNA
IB α-actin
IB SM22
IB β-actin
55
55
25
55
S W S W S W

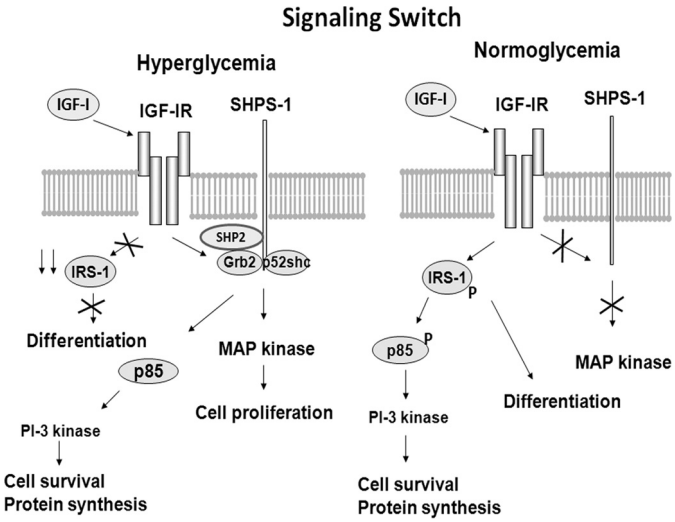

FIGURE 8. **Signaling switch between hyperglycemia and normoglycemia.** During hyperglycemia, IRS-1 is down-regulated, and a signaling complex that includes SHP-2, p52shc, and Grb2 localizes on SHPS-1 in response to IGF-I receptor-mediated SHPS-1 tyrosine phosphorylation. This leads to MAPK and PI3K activation as well as specific pathophysiologic changes in vascular cell function. During normoglycemia, IGF-I signaling is mediated via the IRS-1/PI3K-dependent pathway, and the SHPS-1 signaling complex is not assembled. An important function of IRS-1 is to maintain vascular smooth muscle cell differentiation.

regulation of insulin/IRS-1 signaling in response to cytokines is mediated through SHPS-1.

Unlike IGF-I, peptide growth factors, such as PDGF, that are potent stimuli of VSMC proliferation down-regulate IRS-1 expression even during normoglycemia (27). Similarly, loss of insulin receptor signaling through genetic manipulation results in decreased IRS-1 activation and leads to enhanced serum stimulation of smooth muscle cell proliferation (28). A prior study demonstrated that mice that were globally heterozygous for IRS-1 were more sensitive to vascular dysfunction in the presence of genetically induced lipoprotein excess (29). However, in those mice, the change in IRS-1 was present in multiple cell types that contribute to atherogenesis, including endothelial cells and macrophages as well as smooth muscle cells. In contrast, our study clearly demonstrates that a cell-autonomous reduction of IRS-1 results in markedly altered intracellular signaling, VSMC dedifferentiation, and abnormal proliferation, suggesting that these changes enhance cellular sensitivity to IGF-I stimulation by a mechanism that is independent of changes in these other cell types.

The key finding in this study is that IRS-1 is functioning to inhibit dedifferentiation and, thereby, maintain VSMCs in the differentiated state. This appears to be mediated by its ability to attenuate the expression of KLF-4, a transcription factor that induces smooth muscle cell dedifferentiation (30). Suppression of KLF-4 resulted in maintenance of myocardin expression, which is essential for smooth muscle cell differentiation (13). Myocardin suppression may also regulate the proliferative response to injury because myocardin expression was robust in wild-type animals but nearly absent in IRS-$1^{-/-}$ animals that had a hyperproliferative response to injury, and myocardin is known to modulate this response (31). Other variables, such as TNFα, PDGF, and oxidized LDL, that regulate VSMC differentiation stimulate KLF-4 expression, thereby resulting in enhancement of VSMC dedifferentiation (30, 32–33). During vascular injury, KLF-4 is up-regulated, and this is accompanied by dedifferentiation (34–35). This finding was replicated in our study, and we noted an enhanced dedifferentiation response in the absence of IRS-1, suggesting that IRS-1 is also functioning during injury to attenuate smooth muscle cell proliferation by this mechanism. KLF-4 can also be induced by other atherogenic stimuli, such oxidized phospholipids and advanced glycation end products (32–36).

Cyclosporine, which induces KLF-4 expression, also induces smooth muscle cell dedifferentiation (37). In contrast, myocardin overexpression promotes VSMC differentiation and increases the expression of other VSMC marker proteins (38). Factors that inhibit myocardin expression are associated with dedifferentiation (35). Therefore, our finding of loss of myocardin expression in IRS-$1^{-/-}$ mice strongly supports the conclusion that loss of the ability of IRS-1 to suppress dedifferentiation is mediating the abnormal growth-regulatory response.

Although this study was confined to the analysis of vascular smooth muscle cell differentiation and growth, down-regulation of IRS-1 occurs in multiple cell types in the presence of hyperglycemia (4, 14–16). This raises the possibility that IRS-1 could regulate the state of differentiation in other cell types, such as vascular endothelium, podocytes, and pericytes, whose differentiated functions undergo pathophysiologic changes that lead to diabetic complications (39). Therefore, the reduction in IRS-1 that occurs in these cell types because of hyperglycemia or insulin resistance could lead to abnormal angiogenesis or podocyte dysfunction (40–41). New strategies that focus on ways of controlling this dysregulation of IRS-1 expression hold promise for developing medical treatments that reverse or stabilize the development of these diabetic complications.

Experimental Procedures

Human IGF-I was a gift from Genentech (South San Francisco, CA). Immobilon-P membranes, antibodies against IRS-1 (catalog no. 05-1085) and SHP-2 (catalog no. 06-118) were purchased from EMD-Millipore (Billerica, MA). Antibodies against phospho-AKT (Ser-473) (catalog no. 9271) and phospho-Erk1/2 (catalog no. 4370) were purchased from Cell

FIGURE 7. **Smooth muscle-specific knockout of IRS-1 enhances dedifferentiation of smooth muscle cells and AKT/MAPK activation in femoral arteries after injury.** Femoral arterial lysates after injury (*W*) or sham treatment (*S*) from normal wild-type ($WT^{+/+}$ *NG*), diabetic wild-type ($WT^{+/+}$ *HG*), and normal IRS-$1^{-/-}$ (*IRS-*$1^{-/-}$ *NG*) mice were prepared following a procedure described under "Experimental Procedures." *A*, the lysates were immunoblotted (*IB*) with an anti-KLF4 or an anti-myocardin antibody, and the blots were reprobed with an anti-β-actin. The value of each column is the ratio of the mean value ± S.D. of the scanning units for KLF4 or myocardin from 6 mice/group divided by the scanning units of corresponding β-actin, respectively. *B*, the lysates were immunoblotted with an anti-pAKT (Ser-473) or anti-pErk1/2 antibody and reprobed with an anti-β-actin. The value of each column is the ratio of the mean value ± S.D. from 6 mice/group of the scanning units for pAKT or pErk1/2 divided by the scanning units of corresponding β-actin. *C*, the lysates were immunoblotted with an anti-PCNA, anti-α-actin, or anti-SM22 antibody. The blots were reprobed with an anti-β-actin antibody as a loading control. *, $p < 0.05$; **, $p < 0.01$; significant differences between injury and the sham treatment.

Signaling Technology Inc. (Beverly, MA). Anti-phospho-tyrosine (PY99) (catalog no. sc7020), α-actin (catalog no. sc32251), and KLF-4 antibodies (catalog no. sc20691) were purchased from Santa Cruz Biotechnology, Inc. (Santa Cruz, CA). Anti-β-actin antibody (catalog no. A1978) was purchased from Sigma-Aldrich (St. Louis, MO). Antibodies against Ki67 (catalog no. ab66155) and SM22 (catalog no. ab10135) were purchased from Abcam (Cambridge, MA). An anti-myocardin antibody (catalog no. MAB4028) was purchased from R&D Systems (Minneapolis, MN). An anti-PCNA antibody (catalog no. 610664) was purchased from BD Biosciences (San Jose, CA). A rabbit anti-IRS-2 antiserum was raised by our laboratory using a peptide, CLNINKRADAKHKYLIALYT, linked to keyhole limpet hemocyanin as an immunogen (42). A mouse anti-IRS-2 antibody was provided by Dr. White (Harvard Medical School). An anti-SHPS-1 antiserum was prepared as described previously (43). The horseradish peroxidase-conjugated mouse anti-rabbit, goat anti-mouse, and mouse anti-rabbit light chain-specific antibodies were purchased from Jackson ImmunoResearch Laboratories (West Grove, PA). The synthetic peptide YARAAARQARATLTYADLDM (a SHPS-1/SHP-2-disrupting peptide) and YARAAARQARAVQLYAVVSEE (a control peptide) were synthesized by the Protein Chemistry Core Facility at the University of North Carolina at Chapel Hill. The purity and the sequences were confirmed by mass spectrometry. All other reagents were obtained from Sigma-Aldrich unless otherwise stated.

Mice—All mouse experiments were approved by the Institutional Animal Care and Use Committees of the University of North Carolina at Chapel Hill. The floxed IRS-1 mice and floxed IRS-2 mice were provided by Dr. Morris White (Harvard Medical School). They were created on C57BL/6 background mice following the procedures described previously (44–45). To generate smooth muscle-specific knockout mice, floxed IRS-1 (IRS-$1^{fl/fl}$) or floxed IRS-2 (IRS-$2^{fl/fl}$) mice were crossed with SM22-Cre mice (The Jackson Laboratory, Bar Harbor, ME) for four generations to obtain homozygous SM22-Cre+IRS-$1^{fl/fl}$ or SM22-Cre+IRS-$2^{fl/fl}$ mice. Mice were maintained at 22 °C with a 12-h light/dark cycle and given free access to regular chow (2018 Teklad global rodent diet containing 18.6% protein, 6.2% fat, and 3.5% crude fiber) and water. All groups of mice maintained normal nutrient intake and growth during the experiment.

Induction of Hyperglycemia in Mice and Preparation of Tissues for Biochemical Analysis—Hyperglycemia was induced in wild-type (IRS-$1^{fl/fl}$) and smooth muscle specific IRS-2 knockout mice using low-dose streptozotocin (46). All mice had serum glucose concentrations that were >250 mg/dl, and the levels were maintained during the experiments. There were 12 mice/group (wild-type, wild-type with diabetes, and smooth muscle-specific IRS-1 or IRS-2 knockout mice) for the biochemical analyses and Ki67 staining studies, respectively. There were 16 mice/group for the femoral artery injury study and 8 mice/group for sham treatment. IGF-I (1 mg/kg) ($n = 6$) or PBS ($n = 6$) was administered i.p. 15 min before sacrifice for biochemical analyses and 24 h and 15 min before sacrifice for assessment of Ki67 labeling. For the SHPS-1/SHP-2-disrupting cell signaling experiment, the disrupting peptide (2 mg/kg) and control peptide (2 mg/kg) were injected 24 h and 1 h before sacrifice in diabetic wild-type mice ($n = 12$) and IRS-1 knockout mice ($n = 12$), respectively. IGF-I (1 mg/kg) ($n = 6$) or PBS ($n = 6$) was administered i.p. to each group of mice 15 min before sacrifice. In experiments to assess the effect of disrupting SHPS-1/SHP-2 on the expression of differentiation markers, the disrupting or control peptide (2 mg/kg) was injected every 24 h for 5 days in diabetic wild-type mice ($n = 6$) and IRS-1 knockout mice ($n = 6$). The mice were euthanized by injection of ketamine (100 mg/kg)/xylazine (10 mg/kg). The major organs were cleaned by removing the connective tissues and then weighed. The aortic endothelial cells were collected by opening the aorta longitudinally and scraping the inside of the vessel with a scalpel. The cells were pooled from several aortas. For all other biochemical analyses, the aortas were opened longitudinally, the endothelial cells were removed by scraping, and the remaining tissue was homogenized in ice-cold buffer (20 mM Tris, 150 mM sodium chloride, 2 mM EDTA, and 0.05% Triton X-100 (pH 7.4)) using a glass tissue grinder. The lysates were centrifuged at 13,000 × *g* for 15 min. Protein concentrations of tissue extracts were measured using a BCA assay (Thermo Scientific, Rockford, IL). Equal amounts of protein were used in each analysis.

Femoral Artery Injury—The procedures were performed in the Rodent Advanced Surgical Models Core Facility at UNC Chapel Hill. Briefly, 15-week-old mice were anesthetized with inhaled isoflurane and placed in the supine position with their paws fixed on the table and their lower extremities abducted and extended. The femoral vessels were exposed by an ~1-cm longitudinal groin incision and viewed with the aid of a surgical microscope. The segment of the saphenous artery below the branching of the epigastric and femoral arteries was dissected free from the adjacent nerve and vein. The distal portion of the saphenous artery was encircled with a nylon suture, a vascular clamp was placed proximally at the level of the inguinal ligament, and a 0.010 (0.25-mm) diameter angioplasty guide wire (Advanced Cardiovascular Systems) was introduced into the arterial lumen through an arteriotomy made just distal to the suture. After release of the clamp, the guide wire was advanced to the level of the aortic bifurcation and immediately pulled back. This process was repeated two additional times to denude the endothelium. The guide wire was then removed, and the arteriotomy site was ligated by tying the previously placed suture. For sham treatment, the procedure was the same but without guide wire treatment. The skin incision was closed with non-absorbable sutures. After surgery, mice were returned back to animal housing and routinely monitored for 3 weeks before being sacrificed for specimen collection.

Histology and Morphometry—The vasculature was cleared by transcardial perfusion with 40 ml of PBS, followed by 40 ml of freshly prepared 4% paraformaldehyde in PBS. Femoral arteries were post-fixed for 24 h in 4% paraformaldehyde at 4 °C. The sections were prepared by the UNC Histology Core Facility. Briefly, tissue samples containing the centermost 10-mm section distal to the inguinal ligament were blocked and embedded in paraffin. Twelve adjacent 8-μm sections were cut every 500 μm, extending through the length of the vessel block. Serial sections from each artery were stained with Masson trichrome elastic stain. Images were captured using Aperio-5072 and/or

Olympus BX61 microscopes. Images were analyzed using ImageJ (1.47N, National Institutes of Health) by measuring 10 points of thickness spaced evenly around the vessel wall for each section in a blinded manner.

Immunohistochemistry—The aortae and femoral arteries from mice were fixed with 4% paraformaldehyde overnight, and paraffin-embedded sections were prepared by the UNC Histology Core facility. An immunohistochemistry paraffin protocol provided by Abcam was followed, and the procedures were described previously for Ki67 and DAPI staining (46–47). A similar procedure was used for α-actin staining. The Ki67-positive and total nuclei in a whole aortic ring were quantified using ImageJ (1.47N, National Institutes of Health) and expressed as the percentage of total nuclei.

For measurement of aortic thickness, sections of aortae from each group of mice were stained with hematoxylin and eosin. Images were captured using an Olympus BX61 microscope. Images were analyzed using ImageJ (1.47N, National Institutes of Health) by measuring 10 points of thickness spaced evenly around the vessel wall for each section in a blinded manner. Total DAPI-stained nuclei in each aortic section from different mice were counted.

Immunoprecipitation and Immunoblotting—The immunoprecipitation and immunoblotting procedures were performed as described previously (48). Immunoprecipitation was performed by incubating 0.5 mg of cell lysate protein with 1 μg of anti-SHPS-1 antibody at 4 °C overnight. Immunoblotting was performed using a dilution of 1:1000 for anti-pAKT (Ser-473), pErk1/2, SM22, α-actin, PCNA, and β-actin antibodies and a dilution 1:500 for anti-KLF-4, IRS-1, IRS-2, and myocardin antibodies. The proteins were visualized using enhanced chemiluminescence (Thermo Fisher Scientific).

Statistical Analysis—The results that are shown in all experiments are representative of at least three independent experiments and expressed as the mean ± S.D. Analysis of variance was applied for all data obtained from *in vivo* studies when multiple points were compared. In addition, repeated measures analysis of variance was used where appropriate. $p < 0.05$ was considered statistically significant.

Author Contributions—G. X. designed and performed many of the experiments. He planned the mouse breeding program and supervised the technical work that was necessary to complete the manuscript. D. R. C. helped with design of the experiments and planning of the studies. He reviewed the data extensively and prepared the manuscript. M. F. W. prepared and provided the floxed IRS-1 mice. C. W. maintains the mouse breeding program and assisted with preparation of the tissues for biochemical and immunohistochemical analysis.

Acknowledgments—We thank Laura Lindsay for help with preparing the manuscript. We thank the UNC Histology Core Facility for preparing the histologic sections. We also thank Dr. Mauricio Rojas (Rodent Advanced Surgical Models Core Facility of the UNC McAllister Heart Institute) for assistance with performing the wounding experiments and technical surgical procedures. In addition, we thank Dr. Howard M. Reisner for help with capturing images using Aperio-5072.

References

1. Nathan, D. M., Cleary, P. A., Backlund, J. Y., Genuth, S. M., Lachin, J. M., Orchard, T. J., Raskin, P., Zinman, B., and Diabetes Control and Complications Trial/Epidemiology of Diabetes Interventions and Complications (DCCT/EDIC) Study Research Group (2005) Intensive diabetes treatment and cardiovascular disease in patients with type 1 diabetes. *N. Engl. J. Med.* **353,** 2643–2653
2. Holman, R. R., Paul, S. K., Bethel, M. A., Matthews, D. R., and Neil, H. A. (2008) 10-year follow-up of intensive glucose control in type 2 diabetes. *N. Engl. J. Med.* **359,** 1577–1589
3. White, M. F. (1998) The IRS-signalling system: a network of docking proteins that mediate insulin action. *Mol. Cell. Biochem.* **182,** 3–11
4. Sun, X. J., Crimmins, D. L., Myers, M. G., Jr., Miralpeix, M., and White, M. F. (1993) Pleiotropic insulin signals are engaged by multisite phosphorylation of IRS-1. *Mol. Cell. Biol.* **13,** 7418–7428
5. Navé, B. T., Ouwens, M., Withers, D. J., Alessi, D. R., and Shepherd, P. R. (1999) Mammalian target of rapamycin is a direct target for protein kinase B: identification of a convergence point for opposing effects of insulin and amino-acid deficiency on protein translation. *Biochem. J.* **344,** 427–431
6. Longobardi, L., Granero-Moltó, F., O'Rear, L., Myers, T. J., Li, T., Kregor, P. J., and Spagnoli, A. (2009) Subcellular localization of IRS-1 in IGF-I-mediated chondrogenic proliferation, differentiation and hypertrophy of bone marrow mesenchymal stem cells. *Growth Factors* **27,** 309–320
7. Ding, M., Xie, Y., Wagner, R. J., Jin, Y., Carrao, A. C., Liu, L. S., Guzman, A. K., Powell, R. J., Hwa, J., Rzucidlo, E. M., and Martin, K. A. (2011) Adiponectin induces vascular smooth muscle cell differentiation via repression of mammalian target of rapamycin complex 1 and FoxO4. *Arterioscler. Thromb. Vasc. Biol.* **31,** 1403–1410
8. Saad, M. J., Araki, E., Miralpeix, M., Rothenberg, P. L., White, M. F., and Kahn, C. R. (1992) Regulation of insulin receptor substrate-1 in liver and muscle of animal models of insulin resistance. *J. Clin. Invest.* **90,** 1839–1849
9. Nemoto, S., Matsumoto, T., Taguchi, K., and Kobayashi, T. (2014) Relationships among protein tyrosine phosphatase 1B, angiotensin II, and insulin-mediated aortic responses in type 2 diabetic Goto-Kakizaki rats. *Atherosclerosis* **233,** 64–71
10. Maile, L. A., Capps, B. E., Ling, Y., Xi, G., and Clemmons, D. R. (2007) Hyperglycemia alters the responsiveness of smooth muscle cells to insulin-like growth factor-I. *Endocrinology* **148,** 2435–2443
11. Radhakrishnan, Y., Shen, X., Maile, L. A., Xi, G., and Clemmons, D. R. (2011) IGF-I stimulates cooperative interaction between the IGF-I receptor and CSK homologous kinase that regulates SHPS-1 phosphorylation in vascular smooth muscle cells. *Mol. Endocrinol.* **25,** 1636–1649
12. Radhakrishnan, Y., Maile, L. A., Ling, Y., Graves, L. M., and Clemmons, D. R. (2008) Insulin-like growth factor-I stimulates Shc-dependent phosphatidylinositol 3-kinase activation via Grb2-associated p85 in vascular smooth muscle cells. *J. Biol. Chem.* **283,** 16320–16331
13. Zheng, X. L. (2014) Myocardin and smooth muscle differentiation. *Arch. Biochem. Biophys.* **543,** 48–56
14. Ordóñez, P., Moreno, M., Alonso, A., Llaneza, P., Díaz, F., and González, C. (2008) 17β-Estradiol and/or progesterone protect from insulin resistance in STZ-induced diabetic rats. *J. Steroid Biochem. Mol. Biol.* **111,** 287–294
15. Salt, I. P., Morrow, V. A., Brandie, F. M., Connell, J. M., and Petrie, J. R. (2003) High glucose inhibits insulin-stimulated nitric oxide production without reducing endothelial nitric-oxide synthase Ser1177 phosphorylation in human aortic endothelial cells. *J. Biol. Chem.* **278,** 18791–18797
16. Carvalho, E., Jansson, P. A., Nagaev, I., Wenthzel, A. M., and Smith, U. (2001) Insulin resistance with low cellular IRS-1 expression is also associated with low GLUT4 expression and impaired insulin-stimulated glucose transport. *FASEB J.* **15,** 1101–1103
17. Yu, Q., Zhou, N., Nan, Y., Zhang, L., Li, Y., Hao, X., Xiong, L., Lau, W. B., Ma, X. L., Wang, H., and Gao, F. (2014) Effective glycaemic control critically determines insulin cardioprotection against ischaemia/reperfusion injury in anaesthetized dogs. *Cardiovasc. Res.* **103,** 238–247
18. Hançer, N. J., Qiu, W., Cherella, C., Li, Y., Copps, K. D., and White, M. F. (2014) Insulin and metabolic stress stimulate multisite serine/threonine

phosphorylation of insulin receptor substrate 1 and inhibit tyrosine phosphorylation. *J. Biol. Chem.* **289,** 12467–12484
19. Stöhr, O., Hahn, J., Moll, L., Leeser, U., Freude, S., Bernard, C., Schilbach, K., Markl, A., Udelhoven, M., Krone, W., and Schubert, M. (2011) Insulin receptor substrate-1 and -2 mediate resistance to glucose-induced caspase-3 activation in human neuroblastoma cells. *Biochim. Biophys. Acta* **1812,** 573–580
20. Zhang, H., Hoff, H., and Sell, C. (2000) Insulin-like growth factor I-mediated degradation of insulin receptor substrate-1 is inhibited by epidermal growth factor in prostate epithelial cells. *J. Biol. Chem.* **275,** 22558–22562
21. Copps, K. D., and White, M. F. (2012) Regulation of insulin sensitivity by serine/threonine phosphorylation of insulin receptor substrate proteins IRS1 and IRS2. *Diabetologia* **55,** 2565–2582
22. Lee, S., Lynn, E. G., Kim, J. A., and Quon, M. J. (2008) Protein kinase C-ζ phosphorylates insulin receptor substrate-1, -3, and -4 but not -2: isoform specific determinants of specificity in insulin signaling. *Endocrinology* **149,** 2451–2458
23. Thomas, S. S., Dong, Y., Zhang, L., and Mitch, W. E. (2013) Signal regulatory protein-α interacts with the insulin receptor contributing to muscle wasting in chronic kidney disease. *Kidney Int.* **84,** 308–316
24. Lee, J., Xu, Y., Lu, L., Bergman, B., Leitner, J. W., Greyson, C., Draznin, B., and Schwartz, G. G. (2010) Multiple abnormalities of myocardial insulin signaling in a porcine model of diet-induced obesity. *Am. J. Physiol. Heart Circ. Physiol.* **298,** H310–319
25. Taniyama, Y., Hitomi, H., Shah, A., Alexander, R. W., and Griendling, K. K. (2005) Mechanisms of reactive oxygen species-dependent downregulation of insulin receptor substrate-1 by angiotensin II. *Arterioscler. Thromb. Vasc. Biol.* **25,** 1142–1147
26. Ueki, K., Kondo, T., and Kahn, C. R. (2004) Suppressor of cytokine signaling 1 (SOCS-1) and SOCS-3 cause insulin resistance through inhibition of tyrosine phosphorylation of insulin receptor substrate proteins by discrete mechanisms. *Mol. Cell Biol.* **24,** 5434–5446
27. Zhao, Y., Biswas, S. K., McNulty, P. H., Kozak, M., Jun, J. Y., and Segar, L. (2011) PDGF-induced vascular smooth muscle cell proliferation is associated with dysregulation of insulin receptor substrates. *Am. J. Physiol. Cell Physiol.* **300,** C1375–1385
28. Lightell, D. J., Jr, Moss, S. C., and Woods, T. C. (2011) Loss of canonical insulin signaling accelerates vascular smooth muscle cell proliferation and migration through changes in p27Kip1 regulation. *Endocrinology* **152,** 651–658
29. Galkina, E. V., Butcher, M., Keller, S. R., Goff, M., Bruce, A., Pei, H., Sarembock, I. J., Sanders, J. M., Nagelin, M. H., Srinivasan, S., Kulkarni, R. N., Hedrick, C. C., Lattanzio, F. A., Dobrian, A. D., Nadler, J. L., and Ley, K. (2012) Accelerated atherosclerosis in Apoe$^{-/-}$ mice heterozygous for the insulin receptor and the insulin receptor substrate-1. *Arterioscler. Thromb. Vasc. Biol.* **32,** 247–256
30. Liu, Y., Sinha, S., McDonald, O. G., Shang, Y., Hoofnagle, M. H., and Owens, G. K. (2005) Kruppel-like factor 4 abrogates myocardin-induced activation of smooth muscle gene expression. *J. Biol. Chem.* **280,** 9719–9727
31. Talasila, A., Yu, H., Ackers-Johnson, M., Bot, M., van Berkel, T., Bennett, M. R., Bot, I., and Sinha, S. (2013) Myocardin regulates vascular response to injury through miR-24/-29a and platelet-derived growth factor receptor-β. *Arterioscler. Thromb. Vasc. Biol.* **33,** 2355–2365
32. Pidkovka, N. A., Cherepanova, O. A., Yoshida, T., Alexander, M. R., Deaton, R. A., Thomas, J. A., Leitinger, N., and Owens, G. K. (2007) Oxidized phospholipids induce phenotypic switching of vascular smooth muscle cells *in vivo* and *in vitro*. *Circ. Res.* **101,** 792–801
33. Ali, M. S., Starke, R. M., Jabbour, P. M., Tjoumakaris, S. I., Gonzalez, L. F., Rosenwasser, R. H., Owens, G. K., Koch, W. J., Greig, N. H., and Dumont, A. S. (2013) TNF-α induces phenotypic modulation in cerebral vascular smooth muscle cells: implications for cerebral aneurysm pathology. *J. Cereb. Blood Flow Metab.* **33,** 1564–1573
34. Berk, B. C., Abe, J. I., Min, W., Surapisitchat, J., and Yan, C. (2001) Endothelial atheroprotective and anti-inflammatory mechanisms. *Ann. N.Y. Acad. Sci.* **947,** 93–109; discussion 109–111
35. Yoshida, T., Yamashita, M., Horimai, C., and Hayashi, M. (2013) Smooth muscle-selective inhibition of nuclear factor-κB attenuates smooth muscle phenotypic switching and neointima formation following vascular injury. *J. Am. Heart Assoc.* **2,** e000230
36. Yoshida, T., Gan, Q., and Owens, G. K. (2008) Kruppel-like factor 4, Elk-1, and histone deacetylases cooperatively suppress smooth muscle cell differentiation markers in response to oxidized phospholipids. *Am. J. Physiol. Cell Physiol.* **295,** C1175–C1182
37. Garvey, S. M., Sinden, D. S., Schoppee Bortz, P. D., and Wamhoff, B. R. (2010) Cyclosporine up-regulates Kruppel-like factor-4 (KLF4) in vascular smooth muscle cells and drives phenotypic modulation *in vivo*. *J. Pharmacol Exp. Ther.* **333,** 34–42
38. Raphel, L., Talasila, A., Cheung, C., and Sinha, S. (2012) Myocardin overexpression is sufficient for promoting the development of a mature smooth muscle cell-like phenotype from human embryonic stem cells. *PLoS ONE* **7,** e44052
39. Thum, T., Haverich, A., and Borlak, J. (2000) Cellular dedifferentiation of endothelium is linked to activation and silencing of certain nuclear transcription factors: implications for endothelial dysfunction and vascular biology. *FASEB J.* **14,** 740–751
40. Cester, N., Rabini, R. A., Salvolini, E., Staffolani, R., Curatola, A., Pugnaloni, A., Brunelli, M. A., Biagini, G., and Mazzanti, L. (1996) Activation of endothelial cells during insulin-dependent diabetes mellitus: a biochemical and morphological study. *Eur. J. Clin. Invest.* **26,** 569–573
41. Gödel, M., Hartleben, B., Herbach, N., Liu, S., Zschiedrich, S., Lu, S., Debreczeni-Mór, A., Lindenmeyer, M. T., Rastaldi, M. P., Hartleben, G., Wiech, T., Fornoni, A., Nelson, R. G., Kretzler, M., Wanke, R., *et al.* (2011) Role of mTOR in podocyte function and diabetic nephropathy in humans and mice. *J. Clin. Invest.* **121,** 2197–2209
42. Maile, L. A., Busby, W. H., Sitko, K., Capps, B. E., Sergent, T., Badley-Clarke, J., and Clemmons, D. R. (2006) Insulin-like growth factor-I signaling in smooth muscle cells is regulated by ligand binding to the 177CYDMKTTC184 sequence of the β3-subunit of αVβ3. *Mol. Endocrinol.* **20,** 405–413
43. Maile, L. A., and Clemmons, D. R. (2002) Regulation of insulin-like growth factor I receptor dephosphorylation by SHPS-1 and the tyrosine phosphatase SHP-2. *J. Biol. Chem.* **277,** 8955–8960
44. Dong, X. C., Copps, K. D., Guo, S., Li, Y., Kollipara, R., DePinho, R. A., and White, M. F. (2008) Inactivation of hepatic Foxo1 by insulin signaling is required for adaptive nutrient homeostasis and endocrine growth regulation. *Cell Metab.* **8,** 65–76
45. Lin, X., Taguchi, A., Park, S., Kushner, J. A., Li, F., Li, Y., and White, M. F. (2004) Dysregulation of insulin receptor substrate 2 in β cells and brain causes obesity and diabetes. *J. Clin. Invest.* **114,** 908–916
46. Maile, L. A., Capps, B. E., Miller, E. C., Aday, A. W., and Clemmons, D. R. (2008) Integrin-associated protein association with SRC homology 2 domain containing tyrosine phosphatase substrate 1 regulates igf-I signaling *in vivo*. *Diabetes* **57,** 2637–2643
47. Xi, G., Shen, X., Maile, L. A., Wai, C., Gollahon, K., and Clemmons, D. R. (2012) Hyperglycemia enhances IGF-I-stimulated Src activation via increasing Nox4-derived reactive oxygen species in a PKCζ-dependent manner in vascular smooth muscle cells. *Diabetes* **61,** 104–113
48. Xi, G., Shen, X., and Clemmons, D. R. (2008) p66shc negatively regulates insulin-like growth factor I signal transduction via inhibition of p52shc binding to Src homology 2 domain-containing protein tyrosine phosphatase substrate-1 leading to impaired growth factor receptor-bound protein-2 membrane recruitment. *Mol. Endocrinol.* **22,** 2162–2175